MODELLING OF PLANE STRAIN DEFORMATION OF {100}<001>/{110}<011>-ORIENTED ALUMINIUM BICRYSTAL

WOJCIECH WAJDA, HENRYK PAUL

Instytut Metalurgii i Inżynierii PAN, ul. W. Reymonta 25, 30-059 Kraków
Corresponding Author: nmwajda@imim-pan.krakow.pl (W. Wajda)

Abstract

The experiment of plain strain aluminium bicrystal compression was carried out in order to study material behaviour at grains border of crystallites of cube{100}<001> and hard{110}<011> orientations. In addition, the computer simulation of the bicrystal plain strain compression was performed to support experimental investigation. Both results, from experiment and simulation were consistent. The material data for aluminium single crystal plasticity model were obtained by inverse technique. The goal function for material parameters optimisation is an error of calculated by Finite Element (FE) software force referred to measured force during single crystal plain strain compression.

Key words: aluminium, bicrystal, cube orientation, hard orientation, texture

1. INTRODUCTION

The polycrystalline aggregate is composed from many grains randomly oriented. Due to single crystal anisotropy each grain, depending on its orientation, exhibits different strain stress behaviour. Mechanical properties of the polycrystalline specimen are result, among others, of orientation of all grains and its mutual interaction in the material. In addition there is a tendency observed experimentally to accumulate deformation close to grain boundary of differently oriented grains. As a consequence, the highly deformed volumes of the crystal in the case of further metal forming may become privileged places of the nucleation of new recrystallized grains. In order to gain knowledge of material behaviour close to grain border plain strain compression test was performed on aluminium bicrystal. The cube {100}<001> and hard {110}<011> orientations were chosen for investigation. In addition the experimental investigation of deformation was supported by numerical analysis of bicrystal deformation. In order to simulate crystal

behaviour single crystal plasticity model was implemented in commercial ABAQUS Finite Element (FE) software. In this work the case of cube – hard bicrystal was used for validation of the single crystal plasticity model for its further usage with different materials and orientations.

2. BICRYSTAL SAMPLE PREPARATION FOR PLAIN STRAIN COMPRESSION TEST - EXPERIMENT

The bicrystal with controlled orientations was grown from high purity Al (99.998%) by a modified Bridgman technique (horizontal solidification), using split graphite moulds. The dimensions of the bicrystal bars were approximately 15 mm (thickness) x 22 mm (width) x 150 mm (length). Samples of 15 mm height, 15 mm length and 10 mm width were sectioned from a bar and plane strain compressed at a nominal strain rate of $\sim 10^{-4} s^{-1}$. Teflon films were used as a lubricant and periodically replaced at strain intervals of about 0.2. To favour deformation banding and reduce dynamic recovery

effects the tests were performed at 77 K by immersing the channel-die device in a reservoir with liquid nitrogen. This procedure gives, at relatively low strains, a work-hardened structure containing clearly defined bands.

The cube – hard {100}<001>/{110}<011> bicrystal configuration was used in channel-die compression test in order to study the effect of misorientation between grains on material hardening and strain localization ({hkl}<uvw> signify the compression plane of normal ND and the elongation direction ED respectively). The channel die test was carried out at Laboratory of Institute of Metallurgy and Material Science of Polish Academy of Sciences. The position of the bicrystal in the channel-die device and the nominal orientations of the grains are shown in figure 1.
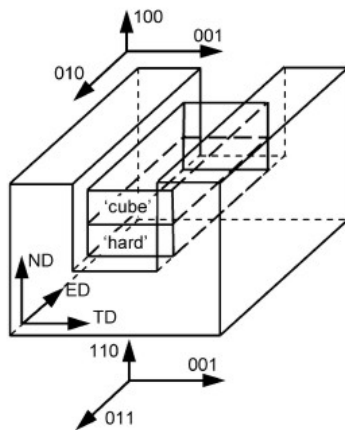
Fig. 1. Schematic bicrystal configuration during channel-die compression showing the grain boundary location and the 'cube – hard' grains orientation.

The interrelation between the grains orientations forming the bicrystal, could be described by the relations:

$$\{100\}<001>/\{110\}<011> \Rightarrow \{100\}<001>$$
$$45^{\circ}<100>\|TD \Leftrightarrow \{110\}<011>$$

where: TD is the transverse direction. The deformation geometry of the bicrystal is such that the boundary separating the top and bottom crystallites at specimen mid-thickness lay parallel to the compression plane.

3. INVESTIGATION OF LOCAL DEFORMATION AFTER PLAIN STRAIN COMPRESSION - MICROSTRUCTURE AND LOCAL ORIENTATION MEASUREMENTS

The deformation microstructures were characterized over a wide range of scales using a combination of transmission electron microscopy (TEM), scan-

ning electron microscopy (SEM) and optical metallography. The samples were sectioned in the ND-ED plane by wire cutting. For thin foil preparation a twinset electropolishing technique was used in standard nitric acid–methanol solution. Optical microscopy was carried out using polarized light on electropolished and lightly anodized (in 2% fluoroboric acid solution) sections. The majority of the metallographic observations were made on the longitudinal plane, i.e. ND-ED. The orientations of the crystallites composing the bicrystals were checked by the X-ray back reflexion Laue method. The deformed specimens were mostly examined by scanning electron microscopy (SEM) in a JEOL JSM 6500F, equipped with a field emission gun (FEG) and electron backscattered diffraction (EBSD) facilities, in which microscope control, pattern acquisition and solution were performed with the HKL Channel 5^{TM} system. For more detailed analyses transmission electron microsopy (200 kV Philips TEM CM200) with semi-automatic Kikuchi pattern analysis, was employed. Local orientation data, obtained by SEM and TEM techniques on the ND-ED section were transformed to the standard ED-TD reference system and presented in the form of {1 1 1} pole figures.

4. SIMULATION OF BICRYSTAL PLAIN STRAIN COMPRESSION

The simplified approach to simulation of bicrystal deformational behaviour was presented in [3], where to describe mechanical properties of each crystallites different flow curve was used obtained in single crystal plain strain compression. The approach is in accordance with the general assumption that aluminium bicrystals deformed up to medium strains behave to a large extent like two individual single crystals [4], however it does not take into account crystallographic aspects of deformation and shear bands formation. In this paper the material model was described by single crystal plasticity model [1]. This allows, in addition to previous approach, take in to consideration and analyse each slip system contribution in global deformation and lattice rotation. In the model the plastic deformation occurs due to crystallographic dislocation slip. Deformation by diffusion, twinning and grain boundary sliding is not taken in to account in the model. The slip on a slip system occurs solely due to acting resolved shear stress on the system. The total deformation gradient (**F**) is composed from two parts:

stretching and rotation ($\boldsymbol{F}^*$) and inelastic gradient ($\boldsymbol{F}^p$), equation (1).

$$\boldsymbol{F} = \boldsymbol{F}^* \cdot \boldsymbol{F}^p \qquad (1)$$

Elastic properties are assumed to be unaffected by the slip, the stress in elastic domain is calculated based on gradient $\boldsymbol{F}^*$. The velocity gradient in the current state decomposed on symmetric rate of stretching ($\boldsymbol{D}$) and antisymmetric spin tensor ($\boldsymbol{\Omega}$), which in turn can be decompose (equation (2)) into lattice parts (superscript *) and plastic part (superscript p).

$$\boldsymbol{D} = \boldsymbol{D}^* + \boldsymbol{D}^p, \quad \boldsymbol{\Omega} = \boldsymbol{\Omega}^* + \boldsymbol{\Omega}^p \qquad (2)$$

The decomposition must satisfy following conditions (equations (3)):

$$\boldsymbol{D}^* + \boldsymbol{\Omega}^* = \dot{\boldsymbol{F}}^* \cdot \boldsymbol{F}^{*-1}, \quad \boldsymbol{D}^p + \boldsymbol{\Omega}^p = \sum_\alpha \dot{\gamma}^{(\alpha)} \boldsymbol{s}^{*(\alpha)} \boldsymbol{m}^{*(\alpha)} \qquad (3)$$

where: $\dot{\gamma}^{(\alpha)}$ is slipping rate on slip system α, $\boldsymbol{s}^{*(\alpha)}$ and $\boldsymbol{m}^{*(\alpha)}$ are respectively slip direction and normal to slip plane in current configuration for slip system α.

In order to relate the slip direction and normal to slip plane in current and reference configuration equations (4) are used.

$$\boldsymbol{s}^{*(\alpha)} = \boldsymbol{F}^* \cdot \boldsymbol{s}^{(\alpha)}, \quad \boldsymbol{m}^{*(\alpha)} = \boldsymbol{m}^{(\alpha)} \cdot \boldsymbol{F}^{*-1} \qquad (4)$$

where: $\boldsymbol{s}^{*(\alpha)}$ and $\boldsymbol{m}^{*(\alpha)}$ are respectively slip direction and normal to slip plane in reference configuration for slip system α.

The crystalline slip in the model is assumed to follow Schmid's law. This implies the slip rate $\dot{\gamma}^{(\alpha)}$ on any slip system depends only on Schmid stress ($\tau^{(\alpha)}$). The Schmid stress depends on current stress state ($\boldsymbol{\sigma}$) and current lattice orientation ($\boldsymbol{s}^{*(\alpha)}, \boldsymbol{m}^{*(\alpha)}$). It is expressed by the definition, equation (5):

$$\tau^{(\alpha)} = \boldsymbol{m}^{*(\alpha)} \cdot \boldsymbol{\sigma} \cdot \boldsymbol{s}^{*(\alpha)} \qquad (5)$$

The amount of shear on a slip system $\dot{\gamma}^{(\alpha)}$ is calculated based on a Schmid law. For rate-dependent crystalline it is determined by following equation (6):

$$\dot{\gamma}^{(\alpha)} = \dot{a}^{(\alpha)} \frac{\tau^{(\alpha)}}{g^{(\alpha)}} \left| \frac{\tau^{(\alpha)}}{g^{(\alpha)}} \right|^{n-1} \qquad (6)$$

Where $\dot{a}^{(\alpha)}$ is reference strain rate on slip system α, $g^{(\alpha)}$ is current strength for slip system α and it is described by equation (7),

$$\dot{g}^{(\alpha)} = \sum_\beta h_{\alpha\beta} \dot{\gamma}^{(\beta)} \qquad (7)$$

The $h_{\alpha\beta}$ is matrix of hardening modules. It describes self and latent hardening of slip systems.

The parameters for the model were obtained by inverse technique. The force measured during the experiment was compared with calculated one by FE model. The parameters of single crystal model were change accordingly to simplex optimisation method until the difference between the forces was mineralised. The same set of parameters was used for each orientation.

5. RESULTS AND DISCUSSION

The investigation of bicrystal behavior during plain strain compression in channel die was carried out twofold. First after each stage of experiment the specimen were carefully investigated by optical microscopy, SEM and TEM techniques. Local orientations and miss-orientations were measured by EBSD technique.

Additionally the investigation was supported by numerical simulation of the test. The crystal plasticity model was used and implemented in to Finite Element (FE) software Abaqus. The calculations were performed at Academic Computer Centre CYFRONET AGH, Kraków (at computer 'baribal', financed from project MNiSW/SGI3700/PAN/ 152/2006).

### 5.1. Local deformation and orientation change measured by SEM and TEM

The bicrystal samples did not deform homogeneously in the channel-die; the top 'cube' grain deformed much more than the bottom 'hard' grain and tended to flow out and over the bottom grain (figure 2).

In 'cube' oriented crystallite the deformation bands are periodically distributed on the longitudinal plane. They run across the whole volume of the crystal and show different inclinations with respect to ED. At relatively low strains most of the substructure is occupied by elongated areas, with a low density of misoriented sub-boundaries, and separated by areas with a high density of dislocation sub-boundary arrays (figure 3). At this stage the bands are clearly rotated by about ±25° around TD [2]. An examples of these microstructures, are presented in figure 3a and b as an Kikuchi band quality maps, with marked grain boundaries of >1° and >15°. At higher strains there are further lattice rotations asso-

ciated with the gradual disappearance of the less misoriented volumes. After 59% reduction the sub-structure is finer than that at 43% reduction, and the areas saturated by sub-grain boundaries tend to occupy a significant part of the 'cube' crystallite.
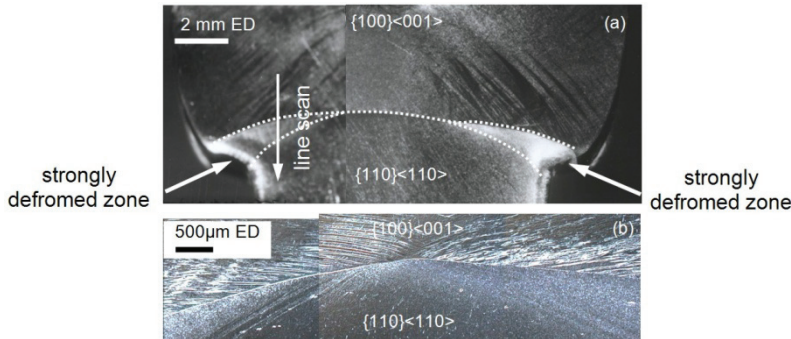
Fig. 2. *(a) Macroscopic changes of the sample shape on the ND-ED longitudinal section. Bicrystal compressed 43%, (b) detail of middle layer (near the grain boundary) within sample deformed 59%.*

For the deformations applied here, 'hard'-oriented crystallite does not show any significant tendency to produce strain heterogeneities (excluding the transition zone at the grain boundary). The orientation spread is nearly the same up to deformations of 59%. The orientation map from the middle layer of the grain, presented in figure 3d shows a nearly uniform distribution of low angle ($>1^{o}$) grain boundaries, in a checker-board pattern. Generally, the {110}<011>-oriented grains deformed to the maximum applied strain did not exhibit deformation banding.
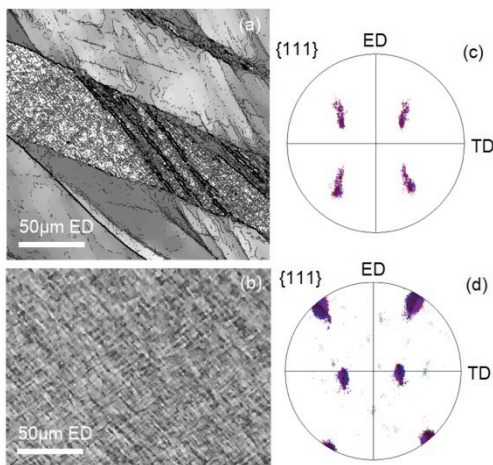
Fig. 3. *Kikuchi band quality map from the areas of: (a) 'cube'-oriented grain and (b) middle part of a 'hard' crystallite and the corresponding {111} pole figures - (c) and (d). SEM/EBSD measurements in ND-ED plane with step size 200nm. Sample deformed 43%.*

Figure 4 shows a TEM microstructure observed along ED near the grain boundary after a thickness reduction of 43%; 'cube' part is composed of nearly regular layers of deformation bands separated by

less dislocated matrix. The typical deformation bands observed here have widths in the range 1-10 μm. Local orientations measured illustrate a characteristic tendency for the lattice rotation reaching 35-40°. The microstructure observed in TEM inside the crystallite with 'hard' orientation, is composed of nearly equiaxed cells with a diameter of 0.3-0.5 μm. Observation in the ND-ED section shows that this sub-structure is formed as a result of the operation of two pairs of slip systems. From a crystallographic point of view it is characterised by a relatively small orientation spread identified along a line scan parallel to ND. The misorientation angle formed between the particular sub-cells only sporadically exceeds 10°.
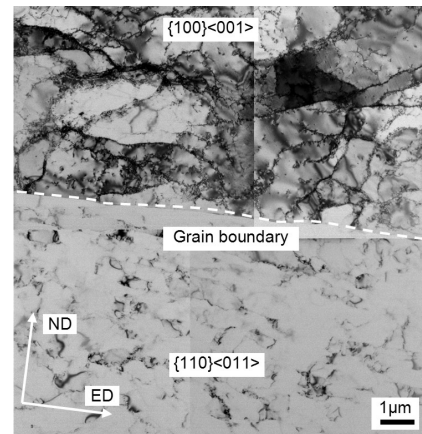
Fig. 4. *TEM bright field image showing microstructure near the grain boundary of sample deformed 43%.*
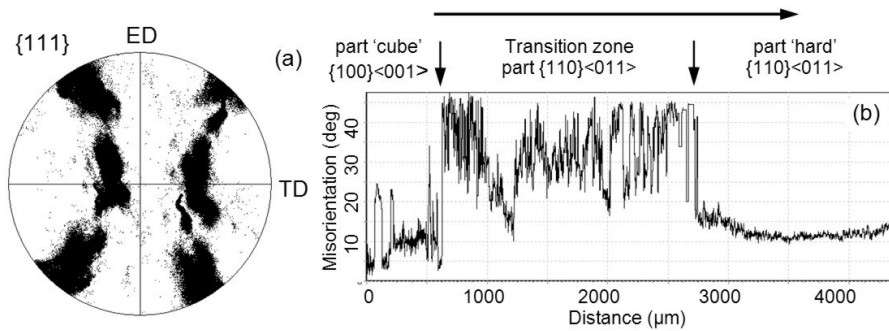
On the longitudinal plane before deformation the bicrystal boundary was a straight line situated along ED. However, during deformation, which induces strong changes of the crystallite shape, bending of the grain boundary occurs (see figure 2). This is especially clearly visible in the 'hard' oriented crystallite, where the volumes lying near the boundary must accommodate the incompatibilities between the neighbouring grains.

The existence of the boundary region indicates that this crystal does not rotate as a whole but splits up into different areas with a broad orientation spread. The {111} pole figure measured on the longitudinal plane (by EBSD method), shown in figure 5a, contains the orientations from a large area of 200μm x 5000μm (longer axis along ED) across the grain boundary and the transition zone (near the free surfaces of the sample). It shows a strong, continuous dispersion of the <111> poles characterized by

strong scattering of the poles by (+/-)TD rotation with some additional rotations around ED and ND axes.

Fig. 5. *a) {111} pole figure showing orientation changes across the grain boundary and transition zone (scan area of 200μm x 5000μm). SEM/EBSD measurements in ND-ED plane with step size 200nm. Sample deformed 59%. b) Misorientation profile with respect to the first point lying within the 'cube' grain across the transition zone.*
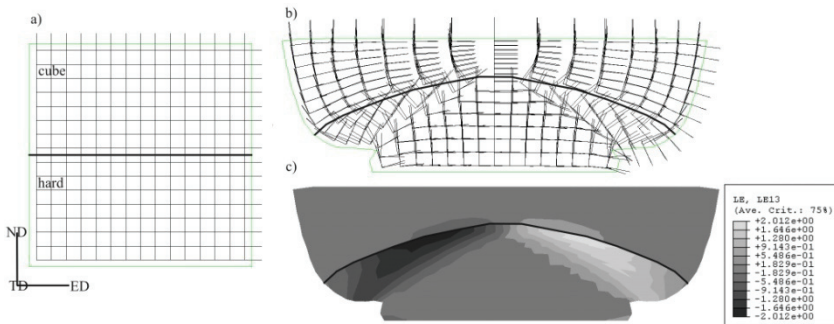
Fig. 6. *a) Initial configuration of simulated aluminum bicrystal (grey line) with marked orientation border (bold black line) and initial position of each element corresponding to global coordinate system (ED, TD, ND), b) local rotation of elements in deformed bicrystal up to 43%, c) shear strain (ε_{13}) distribution after applied 43% deformation.*

The misorientations, calculated with respect to the first measured point lying within the 'cube' grain across the grain boundary, reflect the difference in the structure that is formed (figure 5b). There is only about 12°-15° between the 'hard' grain and the first measured point in the 'cube' grain as a result of the rapid rotation of the 'cube' grain near the transition zone towards the {110}<011> orientation). In the 'cube' crystallite the misorientation angle very often attains values of 25-35°, resulting from the deformation bands. Across the transition region lying near the grain boundary there is a rapid increase and subsequent high amplitude changes of the misorientation angle (up to 40-50°). The regions remote from the boundary in the {110}<011>-oriented crystallite show a gradual disappearance of the orientation variation.

5.2. Numerical simulation of bicrystal plain strain compression – local deformation and orientation changes

In order to investigate the local misorientations, the material model presented in section above was implemented into Abaqus FE software. The simulation of the test was carried out up to near 43% global deformation. To each element set of 12 slip systems were assign by defining proper vectors of slip direction and normal to slip plane representing respectively cube or hard orientation. This approach allows to track local lattice rotation in each element. The changes of lattice orientation are presented in figure 2 a and b.

In figure 6 at each element coordinate system is presented in initial and current (deformed) configuration (specimen). It is seen that the results are in good agreement with the experiment. Large rotations of the lattice are observed at the top corners of hard crystallite. In this area also larger deformation is observed (figure 2 c). The rest of hard crystal is stable (only small rotations are observed). The calculated normals to slip planes in current configuration at the last increment (43% of deformation) were used to construct pole figures (figure 7a). The pole figure is in good agreement with figure 3. The rotation is observed around transverse direction (TD) and extrusion direction (ED). In general the cube crystallite lattice rotates less the hard crystallite.

The different lattice rotation in each crystallites is also clearly seen in figure 7c, where misorientation angle is presented. The angle is referred to calculated orientation at integration point of element marked in figure 7b as reference point. The reference point belongs to crystallite with cube orientation. In addition in figure 7b the elements were misoriantation angle were calculated are marked. In figure 7c it is clearly seen that in hard oriented crystallite the misorientation calculated for particular elements is higher then in cube crystallite, where the

line (misorientation points) are more smooth. This agree with experimental results (see figure 5b).
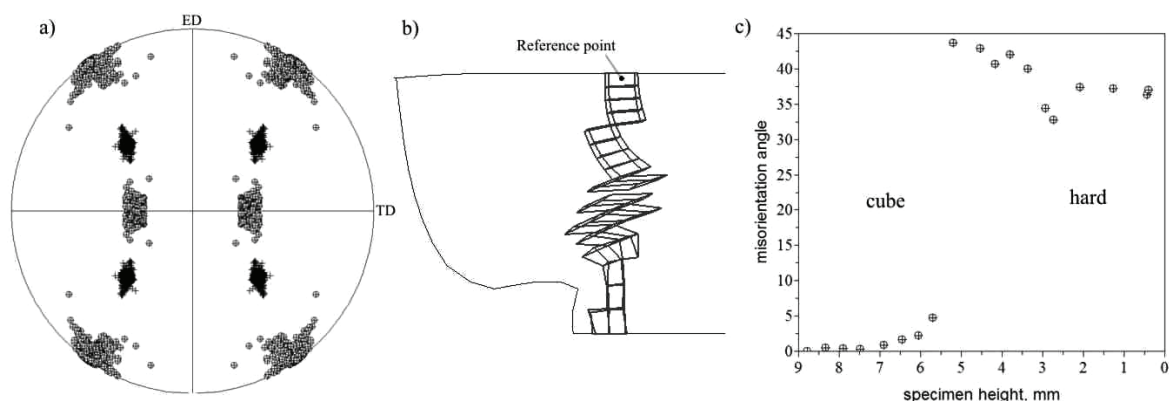
Fig. 7. *a) Pole figure of deformed bicrystal calculated based on results of Finite Element simulation with single crystal plasticity model described above (plus sign – cube orientation, plus sign in circle – hard orientation), b) elements at which misorientation angle were calculated with marked reference point, c) the misorientation angle vs. deformed specimen height.*

6. CONCLUSIONS

Both, calculated pole figures and misorientation angle are very consistent with experimental results. This confirms that the single crystal plasticity model, which takes into account only deformation by slip, is capable to properly describe material behavior with respect of local orientation changes influence on its deformation. The zones of strong deformation agree with the experimental results as well.

REFERENCES

1. Han, C.-S., Gao, H., Huang, Y., Nix, W.D., Mechanism-based strain gradient crystal plasticity–I. Theory, J. Mech. Phys. Solids, 53, 2005, 1188-1203.
2. Paul, H., Driver, J.H., Deformation behaviour of channel-die compressed Al bicrystals with {100}<001>/{110}<011> orientation, Arch. Metall. Mater., 50, 2005, 209-218.
3. Paul, H., Driver, J.H., Wajda, W., Strain hardening and microstructure evolution of channel-die compressed aluminium bicrystals, Mater. Sci. Eng., A 477, 2008, 282–294.
4. Raabe, D., Sachtleber, M., Zhao, Z., Roters, F., Zaefferer, S., Micromechanical and macromechanical effects in grain scale polycrystal plasticity experimentation and simulation, Acta Mater., 49, 2001, 3433–3441.

MODELOWANIE DEFORMACJI BIKRYSZTAŁU ALUMINIUM O ORIENTACJI {100}<001>/{110}<011> W PŁASKIM STANIE ODKSZTAŁCENIA

Streszczenie

W pracy badano mechanizmy deformacji przy granicy ziaren bikryształu aluminium o orientacji {100}<001>/{110}<011> (kubiczna – twarda) odkształconego w płaskim stanie odkształcenia. Analizę zachowania się materiału w pobliżu granicy prowadzono przy pomocy mikroskopii optycznej, skaningowej i transmisyjnej. Otrzymane wyniki porównano z danymi obliczonymi przy pomocy metody elementów skończonych (MES). Do opisu zachowania się materiału wykorzystano model „crystal plasticity", który umożliwił uwzględnienie krystalograficznych aspektów deformacji (orientacji krystalitów, rotacji sieci krystalicznej, itp.).